

Can artificial intelligence (AI) be used to accurately detect tuberculosis (TB) from chest x-ray? A multiplatform evaluation of five AI products used for TB screening in a high TB-burden setting

Authors: Zhi Zhen Qin¹, Shahriar Ahmed², Mohammad Shahnewaz Sarker², Kishor Paul², Ahammad Shafiq Sikder Adel², Tasneem Naheyana¹, Sayera Banu², Jacob Creswell¹

Affiliations:

1. Stop TB Partnership, Geneva, Switzerland
2. International Centre for Diarrhoeal Disease Research, Bangladesh (icddr,b), Dhaka, Bangladesh

Abstract:

Powered by artificial intelligence (AI), particularly deep neural networks, computer aided detection (CAD) tools can be trained to recognize TB-related abnormalities on chest radiographs, thereby screening large numbers of people and reducing the pressure on healthcare professionals. Addressing the lack of studies comparing the performance of different products, we evaluated five AI software platforms specific to TB: CAD4TB (v6), InferRead®DR (v2), Lunit INSIGHT for Chest Radiography (v4.9.0) , JF CXR-1 (v2) by and qXR (v3) by on an unseen dataset of chest X-rays collected in three TB screening center in Dhaka, Bangladesh. The 23,566 individuals included in the study all received a CXR read by a group of three Bangladeshi board-certified radiologists. A sample of CXRs were re-read by US board-certified radiologists. Xpert was used as the reference standard. All five AI platforms significantly outperformed the human readers. The areas under the receiver operating characteristic curves are qXR: 0.91 (95% CI:0.90-0.91), Lunit INSIGHT CXR: 0.89 (95% CI:0.88-0.89), InferReadDR: 0.85 (95% CI:0.84-0.86), JF CXR-1: 0.85 (95% CI:0.84-0.85), CAD4TB: 0.82 (95% CI:0.81-0.83). We also proposed a new analytical framework that evaluates a screening and triage test and informs threshold selection through tradeoff between cost efficiency and ability to triage. Further, we assessed the performance of the five AI algorithms across the subgroups of age, use cases, and prior TB history, and found that the threshold scores performed differently across different subgroups. The positive results of our evaluation indicate that these AI products can be useful screening and triage tools for active case finding in high TB-burden regions.

255 words

Introduction

The improved theoretical understanding in AI technology, the ubiquity of large annotated datasets, and the advance in computer power have fostered a rapid expansion of the AI industry in medical diagnosis(1). Until recently, the most accurate AI methods for image analysis required manual segmentation and computation of specific features annotated by experts. Since the beginning of the decade, deep learning in neural networks is increasingly being used to analyze medical images, such as chest x-rays (CXR)(2, 3).

CXR is recommended by the World Health Organization (WHO) as a screening and triage tool for tuberculosis (TB)(4), a disease which kills more people than any single infectious disease worldwide(5). The use of CXR as a diagnostic tool is limited due to high inter-and intra-reader variability and low specificity (4). For these reasons it was discouraged by WHO as part of TB strategies for many years(6). Additionally, there is a lack of qualified radiologists who can read CXR films in many high TB burden countries (4). However, studies (4, 7-9) have demonstrated the use of CXR as a triage tool to reduce the number of follow on tests required which is a growing concern for numerous active case finding programs. As the number of interventions employing active case finding which screen large numbers of people with CXR has grown in recent years, having the CXR images read quickly to make testing decisions is of great importance (4, 7).

AI technology presents a promising solution to overcome these obstacles. Such technology makes use of neural networks and deep learning to identify TB-related abnormalities on chest radiographs. Inspired by the human nervous system, neural networks are interconnected functions, each comprised of a weight and a bias coefficient. In deep learning, the networks are trained in multiple hidden layers using large sets of known positive and negative cases (ground truth). The networks “learn” by adjusting the weights and biases of the underlying functions based on the difference between predictions and ground truth, a process called back-propagation(10). A complex deep learning network can modify and ‘train’ itself using a large training dataset, enabling it to identify new and unseen data (10).

How exactly deep neural networks detect TB abnormality is unclear, even to those who developed them, and how the networks are constructed are fiercely guarded trade secrets, earning deep neural network the “black box” reputation, i.e. lack of interpretability(10). Furthermore, often the marketed accuracy of AI software is done on the same data superset for training, testing and validation and cannot be generalized to other settings (11).

Several AI companies have emerged in recent years promising to quickly screen digital chest-radiographs to identify people in need of further confirmation testing for TB. While there is evidence that improvements with new versions of software are improving performance (12), current scientific evidence is limited and mostly available for an early version of one product, CAD4TB (Delft Imaging Systems, Netherlands) (9, 13-17). In the last year, two peer-reviewed publications (8, 18) on the performance of other AI software for detecting TB abnormalities with relatively small datasets have been published. WHO has not made a recommendation on the use of automated reading systems for TB due to the current lack of evidence, (4) yet interest in and use of the technology is growing rapidly and more evaluations are required to provide end-users useful analysis to make decisions about different AI solutions. Most evaluations of AI technology for CXR focus on one metric which is the area under the ROC curve (12). However, the possible uses of AI for CXR in TB case finding are varied. A more nuanced evaluation of AI algorithms can better assist both developers to improve their products and end users to decide on product selection. In response to this, we evaluated multiple AI software for TB screening and triage using a large dataset that has not been used to train commercial AI products (4) to help implementers to assess the diagnostic accuracy of these algorithms.

Methods

AI software selection

This evaluation of AI software to read CXR for TB followed the Standards for Reporting of Diagnostic Accuracy (STARD) Initiative on design and conduct of diagnostic accuracy evaluations (19). We identified five AI software platforms with stable version control through the network and the database of innovators developed under the TB REACH initiatives and the Accelerator for

Impact (a4i) project at Stop TB Partnership to include in this study. The software platforms were: CAD4TB (v6), InferRead®DR (v2) by Infervision (China), Lunit INSIGHT for Chest Radiography (v4.9.0) developed by Lunit (South Korea), JF CXR-1 (v2) developed by JF Healthcare (China) and qXR (v3) developed by Qure.ai (India). All AI algorithms produce a continuous abnormality score (from 0 to 100 or from 0 to 1) which represents the probability of presence of TB. Users can set the abnormality or threshold score at any level to decide who should be further evaluated for TB. There is a tradeoff between sensitivity and specificity as the scores change, with the higher the score being the most specific and lower scores being more sensitive.

Sample and image collection

We collected the CXR images from all adults (> 15 years) who presented consecutively to any of the three TB Screening Centres established by icddr,b, with funding from the Stop TB Partnership's TB REACH Initiative, between 15 May 2014 and 4 October 2016. The patients visited the TB centres were mostly referred by private and public health providers or referred from one of the 133 NTP facilities across Dhaka to test for TB. There were also some walk-in clients. After providing informed consent, each participant was verbally screened for TB symptoms, and received a posterior-anterior CXR using digital X-ray machines (Delft EZ DR X-ray). All individuals were asked to submit a sputum sample for testing with the Xpert MTB/RIF assay (Xpert). The Xpert test was repeated if the initial test failed (invalid, error, or no result). The final Xpert results were used as the bacteriological evidence and reference standard in this evaluation.

Image reading

A group of three Bangladeshi, board-certified radiologists (all with MD/ FCPS or both degree in radiology and 10, 6 and 1 years of experience as of 2014) (Table 1) read all the CXR images remotely. Each CXR was read by one of the three Bangladeshi radiologists using the following four categories (definitions in Table 2). The radiologists were blinded to all testing results and clinical and demographic data. They provided standard radiology reports and in addition, graded each CXR image as either highly suggestive of TB, possibly TB, any abnormality, and normal. In addition, we had a sample of all images re-read by US board certified radiologists. The sample

consisted of the CXR images from bacteriologically positive (Bac+) patients who were missed by the Bangladeshi radiologists and missed by different AI products, as well as the image from Bac+ patients that were detected by the Bangladeshi radiologists but missed by different AI products (Supplementary Information, Table 2).

Table 1. Bangladeshi, Board-certified Radiologists

	DEGREE 1	YEAR	DEGREE 2	YEAR	ESTIMATED READS PER YEAR
Radiologist 1	MD	2004	FCPS	2011	17 to 18 thousand
Radiologist 3	MD	2008	-	-	More than 10 thousand
Radiologist 2	MD	2014	-	-	More than 20 thousand

Table 2. Four Categories of Human Reading Categories

CATEGORIES	DEFINITION
a. Highly Suggestive of TB	Highly suggestive of TB only
b. Possibly TB	Including abnormalities highly suggestive of TB and abnormalities possibly associated with TB
c. Any Abnormality	Including abnormality highly suggestive of TB, possible associated with TB and non-TB abnormality
d. Normal	

The five AI algorithms scored the images remotely through Secured File Transfer Protocol from the Stop TB repository except for CAD4TB, which read data that was shared through cloud transfer. All machine reading was performed independently, with the developers blinded to all clinical and demographic data, and ground truth.

Data Analysis

We first compared the performance of the group of three Bangladeshi radiologists and the five AI algorithms, using bacteriological Xpert results as the ground truth. We calculated the sensitivity and specificity of the radiologists' readings for each of the abnormal categories. The threshold scores of each of the AI algorithms were calculated to produce the same dichotomized decisions as the radiologists in terms of sensitivity for each reading category. We then compared

the difference in specificity of the human reading and of the predictions from the five AI algorithms using McNemar test for paired proportions.

We then compared the overall performance of the five AI algorithms using the area under receiver operating characteristic (ROC) curves (AUC), which show the tradeoff between sensitivity and specificity with varying thresholds. However, since the occurrence of TB and not TB is imbalanced (many more negatives than positives), we also calculated the area under Precision-Recall (PRC) curve (PRAUC), which shows precision values for corresponding sensitivity values and is more informative than the ROC curve when evaluating a binary classifier on imbalanced datasets (20).

We proposed a new analytical framework to evaluate screening and triage tests with continuous numeric output, and to better understand threshold selection by factoring in cost efficiency and the ability to triage. We assumed a triage algorithm whereby all adults presenting to the TB centres would be screened by CXR interpreted by each AI algorithm and only those with an abnormality score above a pre-specified threshold would receive the confirmation test by Xpert. We calculated the proportion of subsequent Xpert assays saved as a proxy of cost efficiency of this triage test (with 0% representing the Xpert testing-for-all scenario) and the number of people needed to test (NNT) to find one Bac+ individual indicating the ability to triage. We plotted the sensitivity against the proportion of Xpert saved to show the tradeoff between finding as many Bac+ patients as possible and the cost savings of each AI algorithm. To help our understanding of threshold selection, we produced visualizations between sensitivity, proportion of Xpert saved and NNT with varying threshold scores in a three-way plot. We assessed the distribution of abnormality scores disaggregated by Xpert results and prior history of TB. The Mann-Whitney U test was used to compare non-normal distribution. Finally, since the same threshold scores may provide different results in different populations, we evaluated the performance of the AI algorithms disaggregated by age, prior TB history and use cases using AUC and PRAUC.

Ethics

All enrolled participants provided informed written consent. The study protocol was reviewed and approved by the Research Review Committee and the Ethical Review Committee at the International Centre for Diarrheal Disease Research, Bangladesh (icddr,b).

Role of the AI Developers

The AI developers had no role in study design, data collection, analysis plan, or writing of the study. The developers only had access to the CXR images, and did not receive any of the demographic, symptom, medical, or testing data of the participants.

Results

A total of 24,031 people were consecutively recruited from the three TB centres. Excluding 17 people without a CXR, 138 children younger than 15 years old and 342 individuals who came from community screening or contact tracing, we included 23,566 (98.1%) individuals in this analysis. The median age was 42.0 [30.0, 58.0], 32.9% were female, and almost all (98.5%) reported at least one TB-related symptom. The most common symptoms were cough (89.9%), fever (79.7%), weight loss (63.0%), and shortness of breath (54.7%). Hemoptysis was reported by 3.0% participants. The final sample included 3,538 (15.0%) participants who had a history of prior TB treatment. The prevalence of Bac+ TB confirmed by Xpert was 15.4% overall (n=3,633). Among Bac+ individuals, 4.82% (n=175) were resistant to rifampicin. The radiologists graded 3,619 (15.4%) radiographs as Highly Suggestive of TB, 10,695 (45.4%) radiographs as Possibly TB, 14,282 (60.6%) radiographs as Any Abnormality while 9,284 (39.4%) were read as normal. All images used in this study were taken by Delft Easy DR X-ray System with 50KW X-ray generator Canon CXDI 35x43cm X-ray detector.

More than three quarters (n=17,542, 76.2%) of the participants were referred by public sector or private health providers; 2,992 (13%) participants self-presented (labelled walk in) to the TB centres; and 2,496 (10.8%) participants were first tested in NTP DOTS facilities but had negative

results with smear test and were referred for Xpert testing (Table 3). Across the three groups, the prevalence of Bac+ TB was lowest among walk-ins, n=204 (6.8%), and highest in the NTP DOTS retested subgroup, n=436 (17.5%) (Table 3).

Table 3 Characteristics of the 23,566 individuals included in this study

	Overall N = 23,566	Bacteriological reference		Use cases		
		Bac Positive N = 3,633	Bac Negative N = 19,933	Private & Public Referral N = 17,542	Public DOTS Retesting N = 2,496	Walk In N = 2,992
Age (median [IQR])	42.0 [30.0, 58.0]	37.0 [27.0, 53.0]	43.0 [31.0, 58.0]	44.0 [30.0, 58.0]	37.0 [28.0, 52.0]	38.0 [30.0, 53.0]
Age Group (%)						
Young age (15-25 years)	2621 (11.1)	658 (18.1)	1963 (9.8)	1893 (10.8)	376 (15.1)	287 (9.6)
Middle age (25-60 years)	15779 (67.0)	2349 (64.7)	13430 (67.4)	11423 (65.1)	1777 (71.2)	2239 (74.8)
Old age (≥ 60 years)	5166 (21.9)	626 (17.2)	4540 (22.8)	4226 (24.1)	343 (13.7)	466 (15.6)
Gender = Female (%)	7746 (67.1)	1048 (71.2)	6698 (66.4)	5803 (66.9)	971 (61.1)	772 (74.2)
Cough = Yes (%)	21157 (89.9)	3378 (93.1)	17779 (89.3)	15750 (89.9)	2233 (89.5)	2692 (90.1)
Fever = Yes (%)	18771 (79.7)	3164 (87.2)	15607 (78.4)	14128 (80.6)	2090 (83.8)	2151 (72.0)
Short of breath = Yes (%)	12851 (54.7)	2037 (56.1)	10814 (54.4)	9857 (56.3)	1265 (50.7)	1541 (51.7)
Weight Loss = Yes (%)	14823 (63.0)	2744 (75.6)	12079 (60.7)	11240 (64.1)	1726 (69.2)	1525 (51.0)
Hemoptysis = Yes (%)	3063 (13.0)	463 (12.8)	2600 (13.1)	2211 (12.6)	387 (15.5)	384 (12.9)
Any symptom(s) = Yes (%)	23210 (98.5)	3603 (99.2)	19607 (98.4)	17291 (98.6)	2469 (98.9)	2928 (97.9)
Radiologists grading (%)						
Highly suggestive of TB	3619 (15.4)	1414 (38.9)	2205 (11.1)	2835 (16.2)	510 (20.4)	207 (6.9)
Possibly TB	10695 (45.4)	3214 (88.5)	7481 (37.5)	8612 (49.1)	1195 (47.9)	699 (23.4)
Any abnormality	14282 (60.6)	3453 (95.0)	10829 (54.3)	11353 (64.7)	1477 (59.2)	1108 (37.0)
Normal	9,284 (39.4%)	180 (5.0)	9104 (45.7)	6189 (35.3)	1019 (40.8)	1884 (63.0)
TB History = Yes (%)	3538 (15.0)	600 (16.5)	2938 (14.8)	2562 (14.6)	597 (23.9)	294 (9.8)
Xpert positive (%)	3633 (15.4)			2922 (16.7)	436 (17.5)	204 (6.8)
MTB Burden (%)						
Very Low		626 (17.2)		507 (17.3)	74 (17.0)	34 (16.7)
Low		1085 (29.9)		840 (28.7)	160 (36.7)	59 (28.9)
Medium		1282 (35.3)		1046 (35.7)	145 (33.3)	74 (36.3)

High		639 (17.6)		534 (18.2)	57 (13.1)	37 (18.1)
RIF Result (%)						
Detected		174 (4.8)		130 (0.7)	31 (1.2)	11 (0.4)
Not Detected		3444 (94.8)		17401 (99.2)	2463 (98.7)	2979 (99.6)
Indeterminate		14 (0.4)		11 (0.1)	2 (0.1)	1 (0.0)
Use Case (%)						
Private & Public Referral	17542 (76.2)	2922 (82.0)	14620 (75.1)			
Public DOTS Retesting	2496 (10.8)	436 (12.2)	2060 (10.6)			
Walk-in	2992 (13.0)	204 (5.7)	2788 (14.3)			
AI prediction (median [IQR])						
CAD4TB	58.0 [46.0, 77.0]	81.0 [72.0, 89.0]	53.0 [45.0, 71.0]	62.0 [47.0, 78.0]	56.0 [45.0, 76.0]	46.0 [32.0, 56.0]
qXR (%)	24.0 [3.0, 79.0]	89.0 [82.0, 93.0]	12.0 [2.0, 61.0]	36.0 [4.0, 81.0]	21.0 [3.0, 77.0]	3.0 [2.0, 19.0]
Lunit INSIGHT CXR (%)	30.0 [2.0, 87.0]	95.0 [88.0, 97.0]	10.0 [2.0, 76.0]	45.0 [3.0, 88.0]	33.0 [2.0, 88.0]	3.0 [1.0, 24.0]
JF CXR-1 (%)	85.4 [8.3, 99.8]	100 [99.6, 100]	59.2 [5.4, 99.3]	93.6 [13.7, 99.9]	85.4 [7.1, 99.9]	11.0 [2.0, 81.1]
InferReadDR (%)	28.4 [13.6, 65.0]	74.9 [59.3, 83.2]	22.2 [12.6, 54.1]	33.8 [14.8, 66.9]	29.9 [13.3, 68.7]	15.6 [10.7, 29.4]

Comparison between Radiologists' Reading and Prediction of the AI algorithms

Table 4 Comparison of sensitivity and specificity between radiologists' reading and the predictions of the AI algorithms

Bangladeshi Radiologist				AI algorithms			
Composite Human Reader Categories	Sensitivity	Specificity	Product	Threshold Score	Specificity	Specificity Improvement (95%CI)	
Highly Suggestive of TB (including abnormalities highly suggestive of TB only)	38.9%, (37.3-40.5%)	88.9%, (88.5-89.4%)	CAD4TB	84	90.5% (90.1-90.9%)	1.54% (0.94-2.14%)	
			InferReadDR	0.79	94.2% (93.8-94.5%)	5.23% (4.68-5.78%)	
			JF CXR-1	1.00	93.5% (93.1-93.8%)	4.55% (3.99-5.11%)	
			Lunit INSIGHT CXR	0.96	98.0% (97.8-98.1%)	9.02% (8.54-9.50%)	
			qXR	0.91	97.9% (97.7-98.1%)	8.9% (8.45-9.42%)	
Probably TB (including abnormalities highly suggestive of TB and possibly associated with TB)	88.5%, (87.4-89.5%)	62.5%, (61.8-63.1%)	CAD4TB	63	64.8% (64.1-65.4%)	2.32% (1.37-3.27%)	
			InferReadDR	0.37	64.5% (63.8-65.1%)	2.01% (1.06-2.96%)	
			JF CXR-1	0.95	64.1% (63.4-64.7%)	1.62% (0.66-2.57%)	
			Lunit INSIGHT CXR	0.66	70.3% (69.7-71.0%)	7.87% (6.95-8.80%)	
			qXR	0.64	76.7% (76.1-77.2%)	14.2% (13.3-15.1%)	
Any Abnormality (including abnormalities highly suggestive of TB, possibly associated with TB and other non-TB associated abnormalities)	95.0%, (94.3-95.7%)	45.7%, (45.0-46.4%)	CAD4TB	53	51.3% (50.6-52.0%)	5.60% (4.62-6.59%)	
			InferReadDR	0.20	47.5% (46.8-48.2%)	1.80% (0.82-2.78%)	
			JF CXR-1	0.53	49.0% (48.3-49.7%)	3.31% (2.32-4.29%)	
			Lunit INSIGHT CXR	0.07	47.8% (47.1-48.5%)	2.16% (1.17-3.14%)	
			qXR	0.35	63.5% (62.9-64.2%)	17.9% (16.9-18.8%)	

All five AI algorithms performed significantly better than the human readers when we matched sensitivities for identifying different abnormalities in all three reading categories. The improvement in the specificity of each AI algorithm when we selected threshold scores to produce the sensitivity for the different human reading categories are presented in Table 4. The grading of “highly suggestive of TB” by the radiologists had a sensitivity of 38.9% (95%CI: 37.3% - 40.5%) and a specificity of 88.9% (95%CI: 88.5% - 89.4%). All AI algorithms had better specificity at the same sensitivity level and the improvement in specificity ranged from Lunit INSIGHT CXR’s 9.02% (95%CI = 8.54-9.50%) to CAD4TB’s 1.54% (95%CI = 0.94-2.14%). The radiologists’ sensitivity improved for the category “Possibly TB”, 88.5% (95%CI: 87.4% - 89.5%) but with a lower specificity of 62.5% (95%CI: 61.8% - 63.1%). Again, all matched AI software significantly outperformed human readers. qXR had the highest increase in specificity of 14.2% (13.3-15.1%), followed by Lunit INSIGHT CXR, 7.9% (6.95-8.80%). JF CXR-1, InferReadDR and CAD4TB also outperformed the radiologists with statistically significant increases in specificity (between 1.62% and 2.32%). The radiologists had the highest sensitivity, 95.0% (95%CI: 94.3% - 95.7%) using the “any abnormality” classification to triage the follow on Xpert testing. However, the corresponding specificity was 45.7% (95%CI: 45.0% - 46.4%). In this case, the qXR prediction was 17.9% (16.9-18.8%) higher in specificity than the radiologists. The predictions of CAD4TB, JF CXR-1, Lunit INSIGHT CXR and InferReadDR prediction gained 5.60%, 3.31%, 2.16% and 1.8% in specificity respectively (Table 4).

Performance Comparison of the Five AI algorithms

The tradeoffs between sensitivity and specificity of the five AI algorithms can be visualized in the ROC (Figure 1-a) and precision-recall (Figure 1-b) graphs. The AUCs of the ROC curve from high to low are qXR: 0.9079 (95% CI:0.9031-0.9127), Lunit INSIGHT CXR: 0.8861 (95% CI:0.8802-0.892), InferReadDR: 0.8489 (95% CI:0.8425-0.8553), JF CXR-1: 0.8485 (95% CI:0.8422-0.8549), CAD4TB: 0.8226 (95% CI:0.8164-0.8289). We could detect difference in the AUCs amongst all algorithms except between JF CXR-1 and InferReadDR which had AUCs with overlapping confidence interval. Above the 90% sensitivity mark the ROC curves are not significantly different, except qXR which outperforms the other four AI algorithms. The ROC curves and precision recall curves of

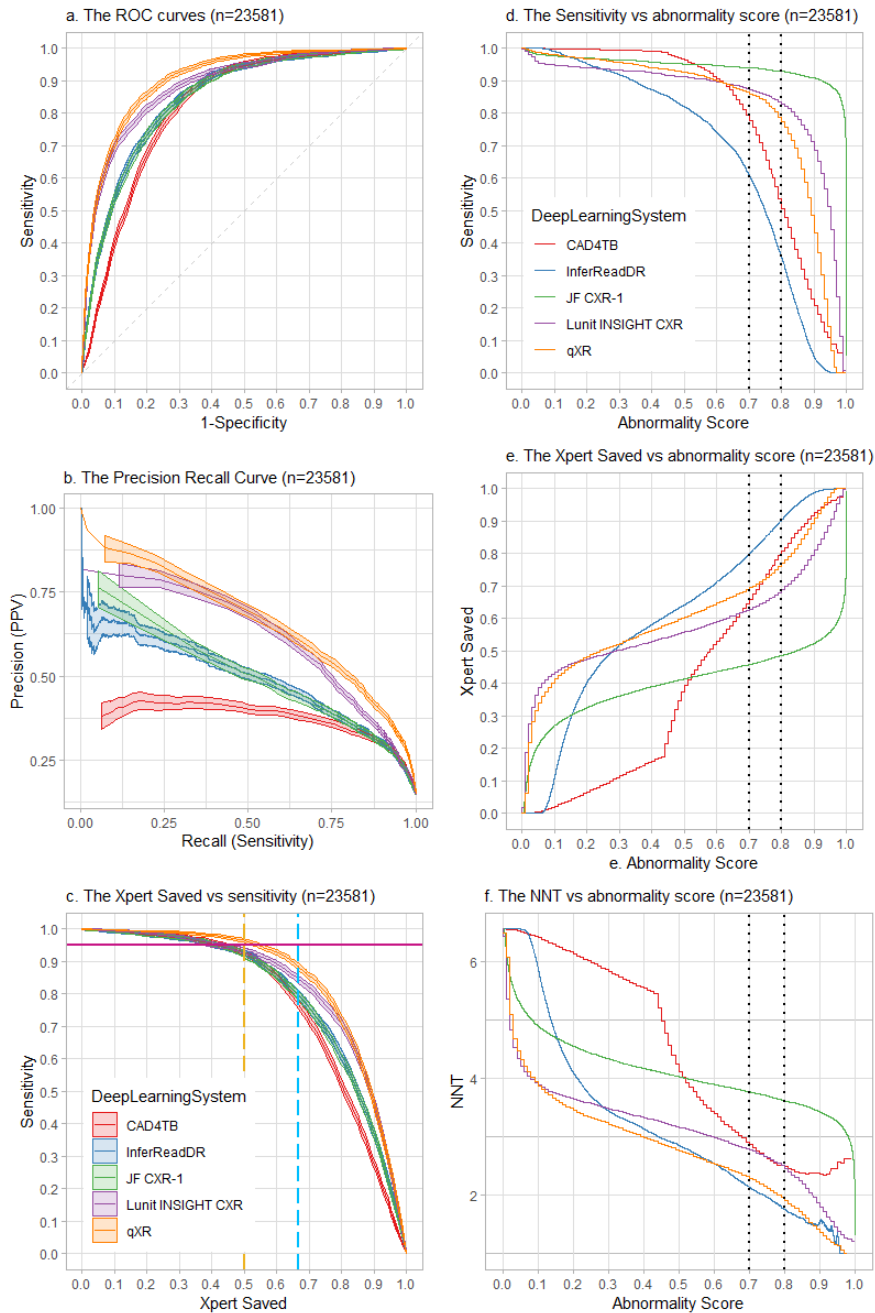
InferReadDR and JF CXR-1 almost completely overlap. The PR curves and the AUC scores (qXR: 0.66, Lunit INSIGHT CXR: 0.62, JF CXR-1: 0.51, InferReadDR: 0.50, CAD4TB: 0.38) showed that some AI classifiers clearly had lower precision values for some given recall values. Unlike ROC, it clearly shows a difference amongst the five AI algorithms.

Figure 1-c shows that all 5 AI algorithms can reduce Xpert testing by at least 50% while maintaining a sensitivity above 90% (yellow dotted line). However, as more follow-on tests are triaged (especially >60%), the difference in the sensitivity of some AI algorithms became statistically significant. In the use case of reducing 2/3 of follow-on Xpert testing (blue dotted line), the sensitivity was lowered to 85%-77% with qXR have the highest sensitivity, followed by Lunit INSIGHT CXR, JF CXR-1, InferReadDR and CAD4TB.

Figure 1 Performance Comparison of the five AI algorithms

a. ROC curves of the five AI algorithms (n=23,566, Bac Pos=3633, Bac Neg=19,933). b. precision recall curves of the five AI algorithms (n=23,566, Bac Pos=3633, Bac Neg=19,933). c. the tradeoff between sensitivity and the proportion of subsequent Xpert test saved. d. The sensitivity of the five AI algorithms with varying threshold cutoff scores. e. the proportion of subsequent Xpert test saved with varying

threshold cutoff scores. F. the number needed to test (NNT) of the five AI algorithms with varying threshold cutoff scores



Although ROC and PR curves indicated that InferReadDR and JF CXR-1 had the same performance, the three-way plot (Figure 1-d to Figure 1-f) showing the dynamics of sensitivity, proportion of

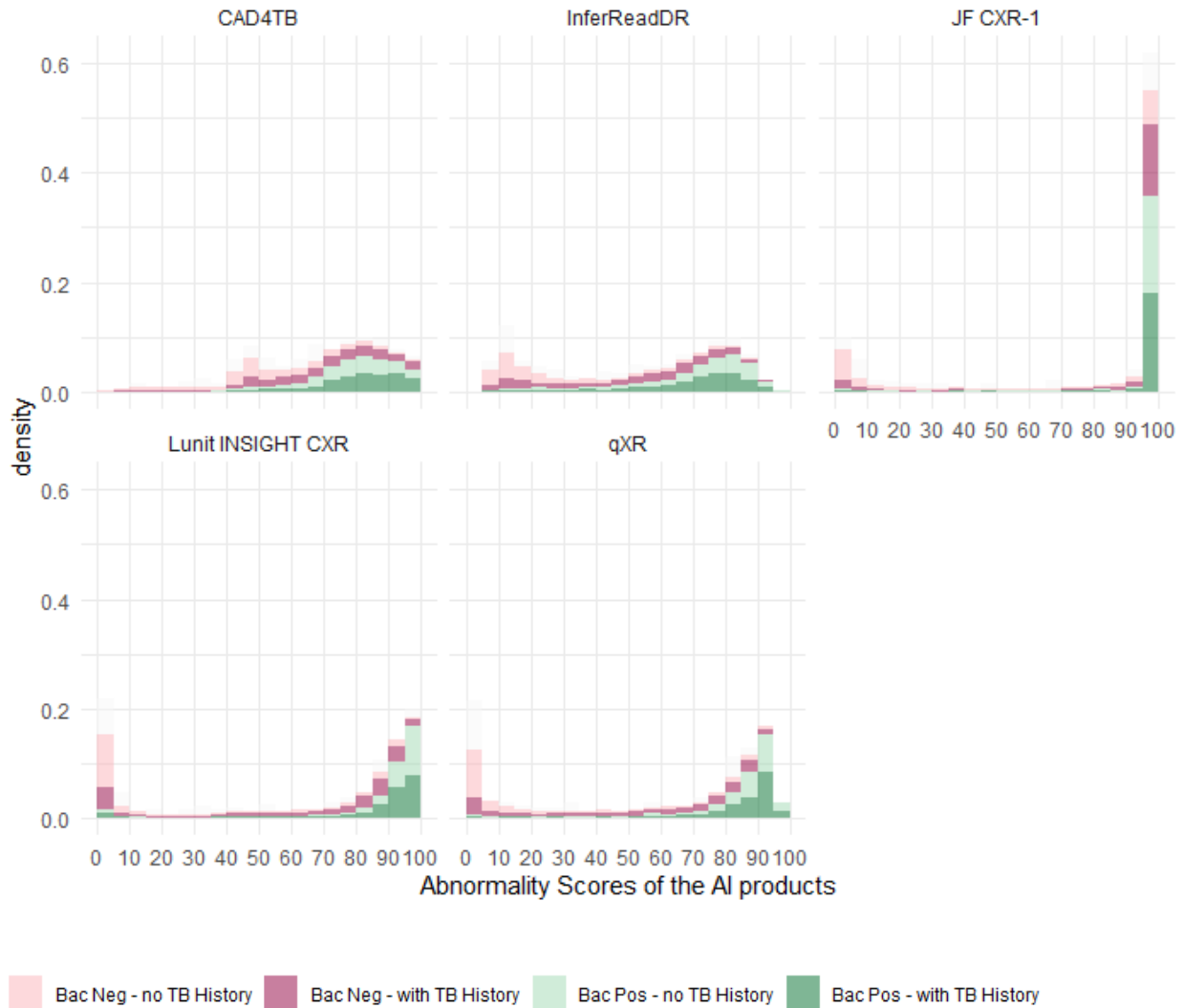
Xpert saved and NNT with varying threshold scores demonstrated that the two systems performed very differently. For most of the decision thresholds (above approximately 0.15), JF CXR-1 had a higher sensitivity, but saved fewer Xpert tests and required higher NNT than InferReadDR. For instance, at 0.8 cutoff threshold, JF CXR-1 is 93.0% (92.1-93.8%) sensitive, can save 48.7% of follow-on Xpert testing, and has NNT of 3.6 (3.5-3.7), compared to InferReadDR with only 35.4% (33.9-37.0%) sensitive, but saved 90.5% of Xpert tests and the NNT was 1.8.

Threshold selection can be informed by checking the performance of a single AI algorithm across the three-way plot (Figure 1-d to Figure 1-f). For most of threshold scores (0-0.9), the sensitivity JF CXR-1 remained above 90% (Figure 1-d), the follow-on Xpert test saved remained between 30% and 60% (Figure 1-e) and the NNT was between 5 and 3 (Figure 1-f). As the cutoff threshold increases from 0 to 0.5, the sensitivity of CAD4TB only slowly decreases to 95% (Figure 1-a), the proportion of Xpert saved increased to 30% (Figure 1-e) and NNT slowly decreases to 5.5 (Figure 1-f) as threshold point reaches 0.5; however a further increases in threshold point from 0.5 results in a sharp decrease in sensitivity and NNT and increases in Xpert saved. The sensitivity of Lunit and qXR remains above around 80% for most of the threshold scores (0-0.8) before quickly decreasing.

The results presented in Figure 1-d demonstrate that there is no decision threshold that is universally applicable to all AI algorithms. For example, the threshold to achieve at least 90% sensitivity for InferReadDR must be below 0.35, below 0.59 for Lunit, 0.60 for CAD4TB and qXR, and anywhere below 0.93 for JF CXR-1.

Figure 2 Stacked density plot of the distributions of the abnormality scores of five AI algorithms disaggregated by Xpert outcomes and by prior TB history.

The dark and light red bars were Bac negative and the dark and light green bars were Bac positive.



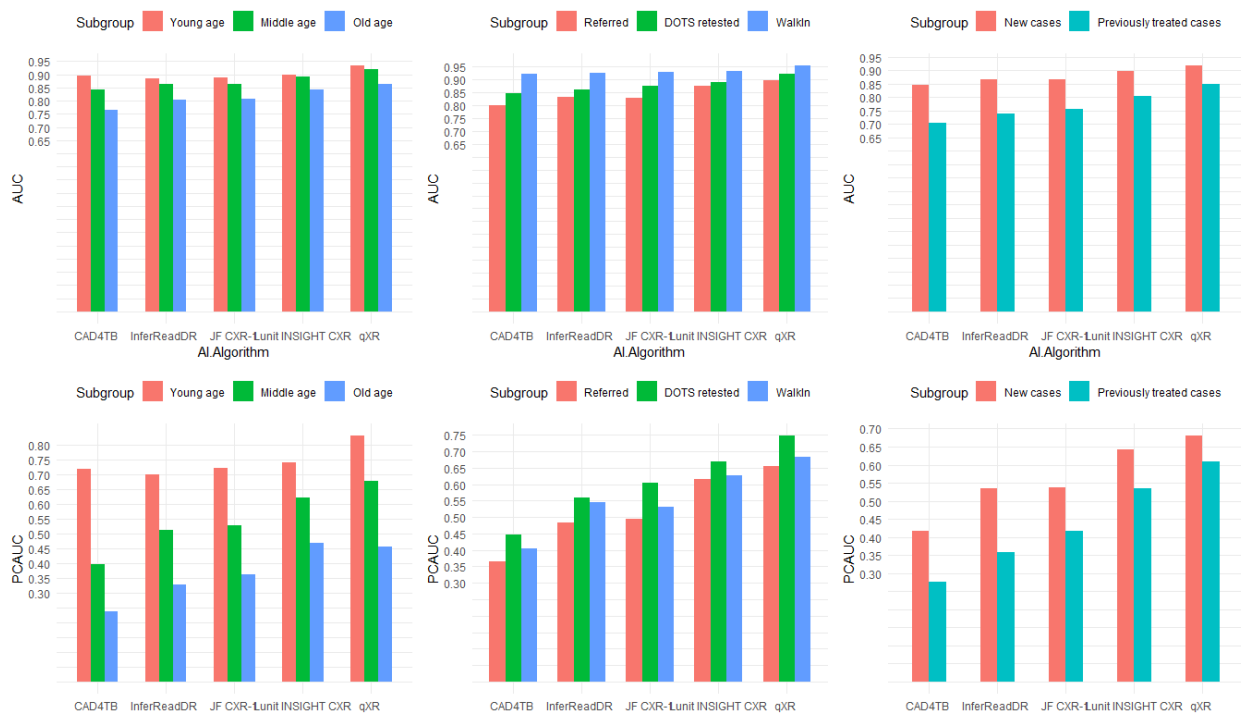
The stacked density plot in Figure 2 shows the distributions of the abnormality scores of the five AI algorithms disaggregated by Xpert outcomes and by prior TB history. The distributions of the five AI algorithms vary considerably, indicating different underlying neural networks and the

effect that changing the threshold scores can have for different products. A perfect test would show Bac- distribution (red bars) should be left skewed and the Bac+ distribution (green bars) would be right skewed with no overlap. Lunit's, qXR's and InferReadDR's density plot demonstrated this dichotomization pattern. Although almost all Bac+ participants received high abnormality scores (95-100) from JF CXR-1, so did many Bac- individuals. None of the distributions of the abnormality scores from the Bac- participants but with prior TB history (the dark red bars) is left skewed (InferReadDR: -0.368, qXR: -0.567, Lunit INSIGHT CXR: -1.44, CAD4TB: -0.55, and JF CXR-1: -0.912).

Subgroup Analysis

Figure 3 The AUCs and PCAUCs of different subgroups. The first row is AUC of ROC curves and the second row is the AUC of PR curves.

Young age (15-25 years old), middle age (25-60 years old), older age (above 60 years old).



We compared the performance of the five AI algorithms across age groups, use cases, and prior TB history using AUC and PRAUC. All five AI algorithms performed worse among the older age

(above 60 years old) than younger age (15-25 years old) and middle age (25-60 years old) (Figure 3). The AI algorithms performed best among walk-in individuals based on AUC. However, using the PRAUC analysis, the algorithms performed best among individuals who were first tested in NTP DOTS facilities but had negative smear results. The AUC and PRAUC were lowest in the subgroup of individuals who were referred by other health providers. Large differences in both AUC and PRAUC were observed in people with and without prior TB history where the software performed better among TB naïve individuals. Due to this, the performance of threshold scores varied by the subgroup tested. For example, a score of 0.5 using Lunit INSIGHT was 92.7% sensitive among people in the older age group and 50.7% specific while the same threshold score produced a sensitivity and specificity of 90.3% and 75.2% for younger people. A CAD4TB score of 65 among people with no TB history produced a sensitivity of 86.7% and a specificity of 70.1% while the same score's performance was 89.8% and 39.7% respectively, in people with prior TB history (data not shown).

US Board Certified Re-reading

The results of the sub-analysis using US board certified radiologists showed that different human readers will capture some cases and miss others. Of the 108 TB cases that were missed by the Bangladeshi radiologists and missed by at least one of the five AI products (at 95% sensitivity), the US board certified radiologists correctly identified 31.5% (n=34) having TB related abnormalities. The US board certified radiologists missed 19.4% (n=54), of the 278 patients detected by the Bangladeshi readers but missed by at least one of the five AI products, while correctly identifying 80.6% (n=224). Out of the 72 TB cases that were missed by the Bangladeshi radiologists but correctly identified by at least one of the AI products (at 95% sensitivity), 60 (91.7%) were correctly identified by the US radiologists (83.4% were graded as having TB abnormality and only 8.3% were graded as normal) (Table 5). The detailed annotations of all the CXRs that were missed by the field readers whereas the AI products were correct, and vice versa, are in Supplementary Information, Table 2.

Table 5 US Board certified radiologists' reading of selected CXRs from bacteriologically confirmed TB patients. Missed by AI products at using 95% Sensitivity thresholds.

	US board certified radiologists						Total
	TB-related Abnormalities		All Abnormalities		Normal		
Bac+ patients missed by the Bangladeshi certified radiologists AND							
missed by 1 AI product	5	41.7%	0	0.0%	7	58.3%	12
missed by 2 AI products	8	61.5%	0	0.0%	5	38.5%	13
missed by 3 AI products	4	25.0%	0	0.0%	12	75.0%	16
missed by 4 AI products	6	28.6%	3	14.3%	12	57.1%	21
missed by 5 AI products	11	23.9%	3	6.5%	32	69.6%	46
Sub-total	34	31.5%	6	5.6%	68	63.0%	108
Bac+ patients detected by the Bangladeshi certified radiologists BUT							
missed by 1 AI product	151	91.0%	12	7.2%	3	1.8%	166
missed by 2 AI products	44	72.1%	12	19.7%	5	8.2%	61
missed by 3 AI products	15	71.4%	5	23.8%	1	4.8%	21
missed by 4 AI products	12	50.0%	5	20.8%	7	29.2%	24
missed by 5 AI products	2	33.3%	1	16.7%	3	50.0%	6
Sub-total	224	80.6%	35	12.6%	19	6.8%	278
Bac+ patients missed by Bangladeshi certified radiologists ONLY	60	83.3%	6	8.3%	6	8.3%	72
Total	318	69.4%	47	10.3%	93	20.3%	458

Discussion

Although how the five AI algorithms were built and what population composition was included in each training set remain unknown to us and the general public, our study shows that the predictions made by the five algorithms significantly outperform experienced Bangladeshi human readers in detecting TB-associated abnormalities. To our knowledge, this is the largest independent study of multiple AI algorithms as a screening and triage tests for TB with CXR and the first published evaluation of JF CXR-1 and InferReadDR for detecting TB. Although the AUCs presented in this study are lower than those in a previous independent evaluation (8), both studies demonstrated the AI algorithms have great clinical potential in high TB burden countries which are mostly resource limited and outperform human readers across settings. Notably, the local readers had access to patient clinical and demographic information when making the decisions. By contrast, the AI algorithms only processed the chest radiographs. The AUCs and PRAUCs indicate that all AI algorithms perform very well and qXR and Lunit INSIGHT CXR are the two top performers in detecting TB related abnormalities while CAD4TB had the lowest AUC and PRAUC. JF CXR-1 and InferReadDR have similar performance between Lunit INSIGHT CXR and CAD4TB.

The results of our analysis also demonstrate the importance of looking beyond ROC and even precision recall curves when evaluating a screening or triage test. The ROC curve is almost universally used to describe the performance of AI algorithms for CXR interpretation(12, 17, 21, 22). However, it provides only one statistical measure which comprises the entirety of the test's performance rather than within a specific program, and its appropriateness for evaluation in most health applications screening or triage for TB is not clear given the lower prevalence of TB in most situations (23).

In this study we illustrated a new analytical framework to evaluate screening and triage tests with continuous output, and to understand threshold selection using diagnostic tests saved and NNT to measure the cost efficiency and the ability to triage using AI to read CXR. We observed that automated reading of CXR by each of the AI algorithms before receiving a confirmation Xpert test is highly sensitive and can save large proportions of the subsequent confirmatory tests. The plot

of sensitivity against Xpert saved of the AI algorithms demonstrated that saving up to 50% Xpert tests while maintaining sensitivity above 90% is feasible. In the hypothetical situation discussed in the results where 95% sensitivity is required, the difference between the different AI products in terms of Xpert saved can be large (48% vs 41%). As the sensitivity reduces, we observed that the differences in proportion of Xpert saved is even bigger, which can have significant cost implication for large case finding programs that cannot expect to use the most sensitive threshold scores (9).

Additionally, the three-way plot of sensitivity, Xpert saved and NNT with varying threshold cutoff points indicates the difference in products that may have very similar performance on ROC and precision recall curves. From the three-way plot and the density plot of the distribution of the abnormality scores of the five AI algorithms disaggregated by Xpert results, it is clear that underlying neural networks of the five AI algorithms were constructed very differently and that there is no universal threshold cutoff scores that can be applicable to all AI algorithms. Moreover, even using the same AI algorithm, the density plots of the Bac- individual with prior TB history indicates the algorithms' poor ability to differentiate between old scarring and active lesions, which can lead to excessive recall in this group.

Our results show that users could choose any point between 0 and 0.9 when using JF CXR-1 and, the resulting sensitivity would be above 90%. The threshold selection can be fine-tuned by the requirement of NNT and Xpert saving. For Lunit and qXR, any threshold scores up to 0.8 resulted in sensitivity above 80%, but between 0.8 and 1, the sensitivity was more prone to change with different threshold cutoffs.

The importance of using a more nuanced analytical framework for evaluation can be demonstrated by imagining different hypothetical case finding situations. For a program focused on capturing almost all people with TB and access to many rapid diagnostic tests, to identify at least 95% of Xpert confirmed patients (i.e. 95% sensitivity), qXR would save the most confirmatory Xpert tests (55%), CAD4TB would save 44% Xpert tests, followed by JF CXR-1, Lunit INSIGHT CXR and InferReadDR which would save 43%, 42%, and 41% of subsequent tests respectively (data and all the values plotted in Figure 1-a to Figure 1-f can be found in the

supplementary information). If we imagine another hypothetical case of a large active case finding program using CXR but with a much more limited budget and the need to reduce the numbers of follow-on Xpert tests by 75% compared to testing and accepting reducing sensitivity, qXR would have a sensitivity of 80.6% (79.2-81.8%), and INSIGHT a sensitivity of 76.6% (75.1-77.9%). This is followed by InferReadDR with 69.3% (67.7-70.8%) sensitivity, JF-CXR 1 with 68.5% (67%-70%) sensitivity, and CAD4TB with 63.0% (61.4-64.6%) sensitivity.

Furthermore, our results show that the overall performance of the five AI algorithms were different in different age groups, use cases and prior TB history. We hypothesize that the abnormalities on the chest due to age and prior TB history influenced the classification of active TB. However, the implication is that the threshold scores likely need to be different depending on the population tested and with sub populations despite recommendations this should not be the case(4, 24). In future studies, it may be possible to incorporate demographic and clinical data along with AI abnormality score to generate an individualized risk score for TB and improve performance.

Our results document the performance of these five algorithms at one point in time. It is important to note that in a few years CAD4TB has produced 6 different versions each with improved performance (25). Since late 2019, when an evaluation of qXR V2 was used, Qure.ai has released V3. Two companies included in this evaluation with good performance had not been evaluated at all in peer reviewed journals. There are a number of other products that are in different stages of certification that may be viable alternatives in the coming months.(cite website) Unlike traditional diagnostic tests which take years to produce and update, the performance of AI improves incredibly fast. This means that future guidance on the use of AI from bodies like WHO must prepare for the speed of change to provide useful information to implementers as data from even 12 months ago is out of date. Multiple independent assessments will be needed and the ability to provide up to date information for end-users is critical.

There are a number of limitations in our study. Due to logistic and budgetary constraints, we did not use culture as the reference standard, meaning that some people with Xpert-negative, culture-positive TB have incorrectly been labelled as not having TB. Most of the participants

included in the study had at least one TB symptom, limiting our ability to generate the results in asymptomatic individuals which is a use case that needs to be evaluated more (4). We did not conduct HIV testing because Bangladesh has a low HIV prevalence (5) but the performance among different sub-populations, especially among people living with HIV who often present with atypical radiological images needs to be better documented (26). Another limitation of our study is that each CXR was read by one Bangladeshi radiologist, not by a panel of radiologists nor by radiologists from different countries. However, the intended use of these AI algorithms is in resource constrained settings with few or no radiologists and neither resources nor time permitted multiple readings of high numbers of images. Lastly, we did not conduct this study prospectively and did not collect implementation data such as programmatic costs, setup, services, user experience, etc.

Conclusions

This independent evaluation addresses the accuracy of five commercially available AI algorithms in triaging patients who need more expensive confirmatory tests for TB by using a large dataset to which developers had no prior exposure. Our results demonstrate that all five AI algorithms outperformed experienced certified radiologists and could save follow-on Xpert testing and reduce NNT while maintain high sensitivity. ROC and precision recall curves are powerful tools for evaluation, however, additional metrics and analysis including our three-way plot of sensitivity, tests saved, and NNT with varying threshold scores will help implementers with threshold and software selection. Future studies should explore the correlation of AI scores and other demographic and contextual data in order to potentially generate more individualized risk scores for optimized performance.

Data Availability

The datasets used in this study can be available upon reasonable request, but images will not be provided to ensure use as an evaluation platform.

Reference

1. Goodfellow I, Bengio Y, Courville A. Deep learning: MIT press; 2016.
2. Chartrand G, Cheng PM, Vorontsov E, Drozdal M, Turcotte S, Pal CJ, et al. Deep learning: a primer for radiologists. Radiographics. 2017;37(7):2113-31.
3. Krizhevsky A, Sutskever I, Hinton GE, editors. Imagenet classification with deep convolutional neural networks. Advances in neural information processing systems; 2012.
4. World Health Organization. Chest radiography in tuberculosis detection: summary of current WHO recommendations and guidance on programmatic approaches. World Health Organization; 2016. Report No.: 9241511508.
5. World Health Organization. Global tuberculosis report 2019: World Health Organization; 2019.
6. Organization WH. What is DOTS?: a guide to understanding the WHO-recommended TB control strategy known as DOTS. World Health Organization; 1999.
7. Creswell J, Qin ZZ, Gurung R, Lamichhane B, Yadav DK, Prasai MK, et al. The performance and yield of tuberculosis testing algorithms using microscopy, chest x-ray, and Xpert MTB/RIF. Journal of clinical tuberculosis and other mycobacterial diseases. 2019;14:1-6.
8. Qin ZZ, Sander MS, Rai B, Titahong CN, Sudrungrot S, Laah SN, et al. Using artificial intelligence to read chest radiographs for tuberculosis detection: A multi-site evaluation of the diagnostic accuracy of three deep learning systems. Scientific reports. 2019;9(1):1-10.
9. Zaidi SMA, Habib SS, Van Ginneken B, Ferrand RA, Creswell J, Khowaja S, et al. Evaluation of the diagnostic accuracy of Computer-Aided Detection of tuberculosis on Chest radiography among private sector patients in Pakistan. Scientific reports. 2018;8(1):12339.
10. Nielsen MA. Neural networks and deep learning: Determination press San Francisco, CA, USA; 2015.
11. Thirona. CAD4TB White paper [updated 2018-08-23. Available from: https://docs.thirona.eu/o/cad4tb/CAD4TB_6.0.0_WhitePaper.pdf.

12. Pande T, Cohen C, Pai M, Ahmad Khan F. Computer-aided detection of pulmonary tuberculosis on digital chest radiographs: a systematic review. *The International Journal of Tuberculosis and Lung Disease*. 2016;20(9):1226-30.
13. Breuninger M, van Ginneken B, Philipson RH, Mhimbira F, Hella JJ, Lwilla F, et al. Diagnostic accuracy of computer-aided detection of pulmonary tuberculosis in chest radiographs: a validation study from sub-Saharan Africa. *PloS one*. 2014;9(9):e106381.
14. Maduskar P, Muyoyeta M, Ayles H, Hogeweg L, Peters-Bax L, van Ginneken B. Detection of tuberculosis using digital chest radiography: automated reading vs. interpretation by clinical officers. *The international journal of tuberculosis and lung disease : the official journal of the International Union against Tuberculosis and Lung Disease*. 2013;17(12):1613-20.
15. Melendez J, Philipson R, Chanda-Kapata P, Sunkutu V, Kapata N, van Ginneken B. Automatic versus human reading of chest X-rays in the Zambia National Tuberculosis Prevalence Survey. *The international journal of tuberculosis and lung disease : the official journal of the International Union against Tuberculosis and Lung Disease*. 2017;21(8):880-6.
16. Philipson RH, Sanchez CI, Maduskar P, Melendez J, Peters-Bax L, Peter JG, et al. Automated chest-radiography as a triage for Xpert testing in resource-constrained settings: a prospective study of diagnostic accuracy and costs. *Scientific reports*. 2015;5:12215.
17. Harris M, Qi A, Jeagal L, Torabi N, Menzies D, Korobitsyn A, et al. A systematic review of the diagnostic accuracy of artificial intelligence-based computer programs to analyze chest x-rays for pulmonary tuberculosis. *PloS one*. 2019;14(9).
18. Nash M, Kadavigere R, Andrade J, Sukumar CA, Chawla K, Shenoy VP, et al. Deep learning, computer-aided radiography reading for tuberculosis: a diagnostic accuracy study from a tertiary hospital in India. *Scientific reports*. 2020;10(1):1-10.
19. Bossuyt PM, Reitsma JB, Bruns DE, Gatsonis CA, Glasziou PP, Irwig LM, et al. Towards complete and accurate reporting of studies of diagnostic accuracy: the STARD initiative. *The Standards for Reporting of Diagnostic Accuracy Group. Croatian medical journal*. 2003;44(5):635-8.
20. Saito T, Rehmsmeier M. The precision-recall plot is more informative than the ROC plot when evaluating binary classifiers on imbalanced datasets. *PloS one*. 2015;10(3).

21. McKinney SM, Sieniek M, Godbole V, Godwin J, Antropova N, Ashrafian H, et al. International evaluation of an AI system for breast cancer screening. *Nature*. 2020;577(7788):89-94.
22. Arcadu F, Benmansour F, Maunz A, Willis J, Haskova Z, Prunotto M. Deep learning algorithm predicts diabetic retinopathy progression in individual patients. *NPJ digital medicine*. 2019;2(1):1-9.
23. Corbett EL, Bandason T, Duong T, Dauya E, Makamure B, Churchyard GJ, et al. Comparison of two active case-finding strategies for community-based diagnosis of symptomatic smear-positive tuberculosis and control of infectious tuberculosis in Harare, Zimbabwe (DETECTB): a cluster-randomised trial. *The Lancet*. 2010;376(9748):1244-53.
24. Nathavitharana RR, Yoon C, MacPherson P, Dowdy DW, Cattamanchi A, Somoskovi A, et al. Guidance for Studies Evaluating the Accuracy of Tuberculosis Triage Tests. *The Journal of infectious diseases*. 2019;220(Supplement_3):S116-S25.
25. Murphy K, Habib SS, Zaidi SMA, Khowaja S, Khan A, Melendez J, et al. Computer aided detection of tuberculosis on chest radiographs: An evaluation of the CAD4TB v6 system. *Scientific reports*. 2020;10(1):1-11.
26. Padyana M, Bhat RV, Dinesha M, Nawaz A. HIV-tuberculosis: A study of chest X-ray patterns in relation to CD4 count. *North American journal of medical sciences*. 2012;4(5):221.